

ORIGINAL ARTICLE

Open Access



Pre-research on Enhanced Heat Transfer Method for Special Vehicles at High Altitude Based on Machine Learning

Chunming Li¹, Xiaoxia Sun^{1*}, Hongyang Gao² and Yu Zhang²

Abstract

The performance of an integrated thermal management system significantly influences the stability of special-purpose vehicles; thus, enhancing the heat transfer of the radiator is of great significance. Common research methods for radiators include fluid mechanics numerical simulations and experimental measurements, both of which are time-consuming and expensive. Applying the surrogate model to the analysis of the flow and heat transfer in louvered fins can effectively reduce the computational cost and obtain more data. A simplified louvered-fin heat transfer unit was established, and computational fluid dynamics (CFD) simulations were conducted to obtain the flow and heat transfer characteristics of the geometric structure. A three-factor and six-level orthogonal design was established with three structural parameters: angle θ , length a , and pitch L_p of the louvered fins. The results of the orthogonal design were subjected to a range analysis, and the effects of the three parameters θ , a , and L_p on the j , f , and JF factors were obtained. Accordingly, a proxy model of the heat transfer performance for louvered fins was established based on the artificial neural network algorithm, and the model was trained with the data obtained by the orthogonal design. Finally, the fin structure with the largest JF factor was realized. Compared with the original model, the optimized model improved the heat transfer factor j by 2.87%, decreased the friction factor f by 30.4%, and increased the comprehensive factor JF by 15.7%.

Keywords Louvered fins, Numerical simulation, Machine learning, Comprehensive performance

1 Introduction

The normal working temperature of the engine of large special vehicles running in a plateau area is usually around 80–90 °C, but due to the harsh climate in such areas, regarding air pressure, oxygen content, etc., coupled with rugged roads, the engine overheats, affecting normal work [1–4]. Further, with the development of “high-power, low-emission, lightweight” automobile engines, besides the application of new power batteries,

motors, and other heat-producing components in cars, requirements regarding the heat dissipation performance of car radiators have increased [5–7].

Therefore, it is important to improve the heat dissipation performance of vehicle radiators to obtain satisfactory performance for special vehicles running in highland areas [8–10].

The cooling technology for automotive louvered radiators has been extensively researched and developed in recent decades [11–13]. Many researchers have studied improved structures and more complex louvered radiators, such as corrugated louvered fins [14, 15], louvered-fin heat exchangers with variable louver angle [16], louvered fins with unequal louver pitches [17], and X-shaped louvered fins [18]. The application of nanofluids in improving the performance of louvered fins has

*Correspondence:

Xiaoxia Sun
sun_xiaoxia1983@163.com

¹ China North Vehicle Research Institute, Beijing 100072, China

² Mechanical Engineering Department, Zhejiang University City College, Hangzhou 310015, China

received considerable attention [19, 20]. In addition, some scholars have examined the effect of the geometric parameters of louvered heat sinks on the flow heat transfer.

Webb et al. [21] conducted a flow visualization study to investigate the characteristics of internal fluid flow under different louver angles, louver pitch angles, and spacing, and proposed the first empirical formula for fluid flow efficiency. Sanders et al. [22] enhanced the heat transfer in a louvered fin heat exchanger using winglets placed on the louvers with optimized parameters, resulting in a 39% enhancement in heat transfer and a 23% increase in the coefficient of friction of the heat exchanger.

Park et al. [23] studied the effect of louvered fin structural parameters on the heat dissipation performance and optimized the louvered fin structure, which improved the heat dissipation performance by 15.7%. Erbary et al. [24] studied the heat dissipation performance and fluid flow properties of the air side of louvered fin radiators at low Reynolds numbers, and the results showed that the best heat dissipation performance was obtained at the Reynolds number of 229 and louvered window opening angle of 20. Hsieh et al. [25] found that the fin spacing is the main factor affecting the heat exchanger thermal performance, and a set of louver structural parameter combinations were obtained via comprehensive evaluation of the index JF maximum.

The main method used to study the heat transfer performance of a louvered fin flow is numerical simulation [26, 27]. However, in flow heat transfer analysis, the time and computational resources consumed are large owing

Table 1 Thermophysical properties of heat sink materials and coolants (mm)

Parameter	Value	Parameter	Value
L_p (mm)	1.2	F_p (mm)	1.5
L_h (mm)	3	T_p (mm)	4.5
F_h (mm)	3.5	F_d (mm)	18.9
D_m (mm)	1	δ (mm)	0.1
S_1 (mm)	0.75	S_2 (mm)	3

to the large amount of simulation calculations, high equipment requirements, long computation time, and the need for a large number of models for simulation and analysis. In contrast, the proxy model uses the samples of the ANSYS numerical simulation as the training data for learning. The performance prediction of the new sample model can be provided instead of a numerical simulation by the agent model that has completed training.

At present, some foreign scholars have already used algorithms such as the genetic algorithm (GA) [28], artificial neural network (ANN) [29], and adaptive neuro-fuzzy inference system (ANFIS) [30] for the calculation, prediction, and optimal design of heat transfer and pressure drop of heat exchangers, and few domestic scholars are currently using machine learning algorithms to optimize vehicle power performance [31–36]. Thus, the purpose of this study was to propose an optimization method for louvered window fin heat exchangers; more specifically, to employ ANN algorithms to optimize the louvered window fin structure and find the optimal fin structural parameters to reduce unnecessary repetitive modeling and simulation, accelerate the optimal design of heat exchangers, and achieve overall optimization with few samples.

In the second section of this paper, we introduce the sources of sample data used for machine learning, including the construction of geometric models, setting of boundary conditions, verification of grid independence, and comparison of experimental data with simulation data. In the next section, the construction of the LMBP model and several important parameters considered to evaluate the effects of machine learning are discussed. In the fourth section of this paper, the prediction results obtained by the ANN are evaluated. The louvered fin structure with the largest JF factor was determined based on the original data and verified.

2 Data Collection and LMBP Modeling

In this section, the sample data used for machine learning and the construction of the LMBP model are introduced.

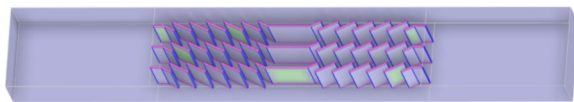


Figure 1 Simplified model of louvered fins

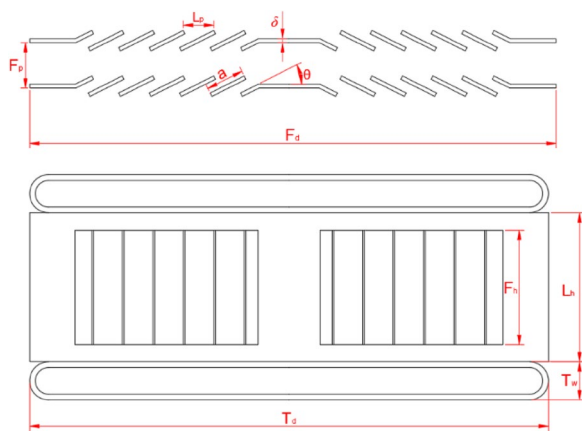


Figure 2 Schematic of structural parameters of the louvered fins

2.1 Geometry Structure

The louvered fin radiator is divided into the gas and water sides, and the gas side is a louvered fin structure. The spacing between the fins was assumed as equal, the louvered fin spacing was also equal, and the angle was kept constant. Because the structure of each louvered fin is the same, only three could be selected for the study. SpaceClaim software was employed to realize a three-dimensional simplified model of the louvered fins, as presented in Figures 1, 2 and Table 1.

The computational domain is divided into fluid domain and solid domain, the solid domain part includes louvered fins and flat tubes; the rest is fluid domain, which is extended by a certain length on both sides to prevent backflow phenomenon in the computational process. The final established louvered fin model computational domain size is 3 mm × 5.7246 mm × 38.9 mm.

The performance of louvered fins mainly includes the heat transfer performance and flow resistance performance, and the performance evaluation indexes of louvered fins at home and abroad are generally the heat transfer factor j and friction factor f [37, 38]. Therefore, in this study, three indices: heat transfer factor j , friction factor f , and JF factor, were selected as the evaluation indices.

2.2 Louvered-Fin Performance Parameter Calculation

The formula for calculating heat exchange of the louvered fins is as follows:

$$Q_f = m_f c_a (T_{aout} - T_{ain}), \quad (1)$$

where, Q_f is the louver fin air side heat exchange; c_a is the specific heat capacity of air; m_f is the louver fin air side mass flow rate; T_{aout} , T_{ain} are the louver air side inlet and outlet temperature respectively

$$h_f = \frac{Q_f}{A_f \Delta T_f}, \quad (2)$$

where, A_f is the total heat transfer area of the louvered fins.

Log mean temperature difference ΔT_f is given by:

$$\Delta T_f = \frac{T_{aout} - T_{ain}}{\ln \frac{T_{fw} - T_{ain}}{T_{fw} - T_{aout}}}, \quad (3)$$

where, T_{fw} is the louvered fin wall temperature.

In the louvered fin radiator, the air on the gas side is considered an incompressible fluid, the density on the air side is treated as a constant, and the air pressure drop ΔP on the gas side of the radiator can be expressed as:

$$\Delta P = P_{in} - P_{out}, \quad (4)$$

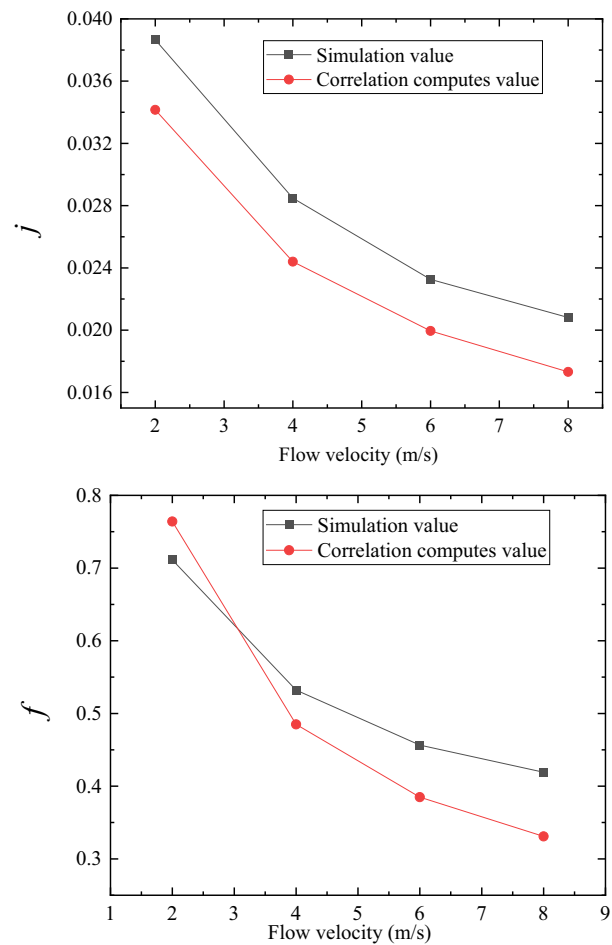


Figure 3 Comparison of simulation results and empirical correlation calculation results

where P_{in} and P_{out} are the pressure at the air inlet and outlet, respectively.

The heat transfer factor j and the resistance factor f are calculated as:

$$j = \frac{h_f}{\rho u_a c_a} \text{Pr}^{\frac{2}{3}}, \quad (5)$$

$$f = \frac{2\Delta P d_e}{\rho u_a^2 L}, \quad (6)$$

where Pr is the Prandtl number, ρ is the air density, u_a is the velocity, and L is the basin length.

The integrated Star River evaluation factor considers both heat transfer and flow resistance. The integrated performance evaluation factor considers both the heat transfer and flow resistance performance, as $JF = j/f^{1/3}$.

The internal flow and heat transfer are quite complex because of the complex structure of louver heat sinks. To

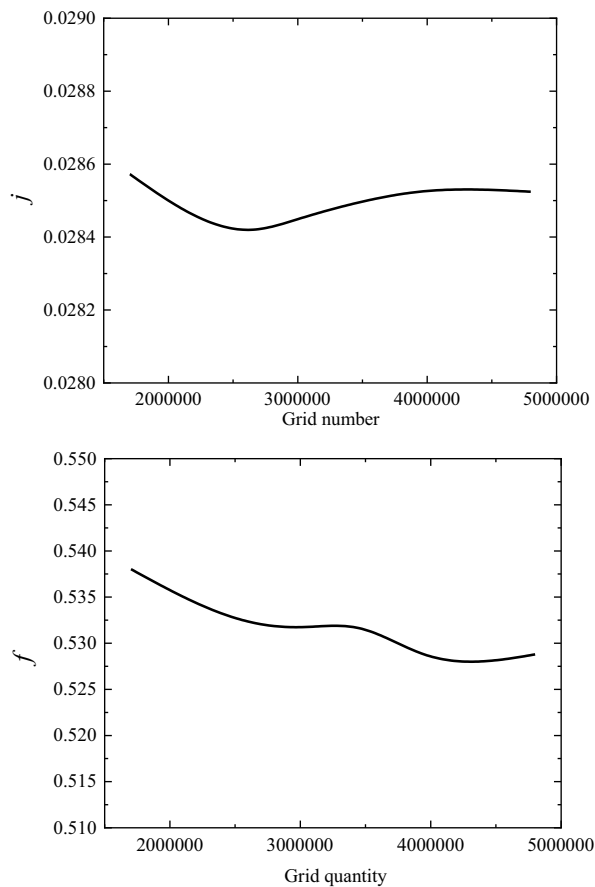


Figure 4 Variation of j factor and f factor with the number of grids

facilitate this study, some assumptions were introduced, as follows:

1. The air flowing through the louvered fins is an incompressible fluid and the physical properties of the air do not change as the temperature increases.
2. The convective heat transfer process between the louvered fins and air is a steady-state process.

3. Owing to the small thickness of the louvered fins, the thermal conductivity can be neglected, and a uniform thickness of these structures can be assumed.
4. The deformation of the fins due to the impact of air can be ignored, so the spacing and angle of the louvered fins remain constant. The effect of gravity on the heat transfer and flow can also be ignored.

Based on the assumptions above, the continuity, momentum, and energy equations for the fluid regions were established to describe the flow and heat transfer characteristics of louver heat sinks, as shown in Eqs. (7)–(9), respectively.

$$\frac{\partial \rho}{\partial t} + \vec{\nabla} \cdot (\rho \vec{u}) = 0, \quad (7)$$

$$\frac{\partial \vec{u}}{\partial t} + (\vec{u} \cdot \vec{\nabla}) \vec{u} = -\frac{1}{\rho} \vec{\nabla} p + \nu \vec{\nabla}^2 \vec{u}, \quad (8)$$

$$\rho c_p \left[\frac{\partial T}{\partial t} + (\vec{u} \cdot \vec{\nabla}) T \right] = k \vec{\nabla}^2 T + \Phi, \quad (9)$$

where ρ is the density of the fluid, t is time, \vec{u} is the velocity vector of the fluid, p is the pressure of the fluid, ν is the kinematic viscosity, c_p is the specific heat capacity, T is the temperature, k is the thermal conductivity, and Φ is the dissipation function.

2.3 Data Validation

In this study, the flow and heat transfer characteristics of louvered fins were investigated using numerical simulations. In addition, to verify the accuracy of the numerical simulation simulations, the results were compared and validated with the calculated results of the well-known Chang-Wang empirical correlation equations [39].

The j factor correlation equation is

$$j = Re_{L_p}^{-0.49} \left(\frac{\theta}{90} \right)^{0.27} \left(\frac{F_p}{L_p} \right)^{-0.14} \left(\frac{F_h}{L_p} \right)^{-0.29} \left(\frac{T_d}{L_p} \right)^{0.68} \left(\frac{T_p}{L_p} \right)^{-0.28} \left(\frac{\delta}{L_p} \right)^{-0.05}, \quad (10)$$

When $Re_{L_p} > 150$, the f factor correlation equation is

Table 2 Factors and levels of orthogonal tests

Level	θ (°)	a (mm)	L_p (mm)
1	16	1.05	0.9
2	19	1.2	1.0
3	22	1.35	1.1
4	25	1.5	1.2
5	28	1.65	1.3
6	31	1.8	1.4

Table 3 Thermophysical properties of heat sink materials and coolants

Materials	Density (kg/m ³)	Thermal conductivity (W/m·K)	Specific heat capacity (J/kg·K)
Air	1.225	0.0242	1006.433
Aluminium	2719	202.4	871

$$f_1 = 4.97 \text{Re}_{L_p}^{0.6049-1.064/\theta^{0.2}} \left\{ \ln \left[\left(\frac{\delta}{F_p} \right)^{0.5} + 0.9 \right] \right\}^{-0.527}, \quad (11)$$

$$f_2 = [(D_h/L_p) \ln(0.3 \text{Re}_{L_p})]^{-2.996} (F_p/L_h)^{-0.7931} (T_p/T_h), \quad (12)$$

$$f_3 = (T_p/D_m)^{-0.0446} \ln [1.2 + (L_p/F_p)^{1.4}]^{-3.553} \theta^{-0.477}, \quad (13)$$

$$f = f_1 \cdot f_2 \cdot f_3, \quad (14)$$

where: Re_{L_p} is the Reynolds number based on louver pitch; θ is the louver angle; F_p is the fin pitch; L_p is the louver pitch; F_h is the fin height; T_d is the flat tube depth; L_h is the louver height; T_p is the flat tube pitch; δ is the fin thickness; D_h is the hydraulic diameter of fin array; D_m is the flat tube diameter; T_h is the difference between the flat tube pitch and the flat tube diameter.

According to the Chang-Wang empirical correlation formula, the heat transfer factor j and friction factor f were calculated, and the simulation results were compared with the correlation calculation results, as shown in Figure 3. From the comparison results, it can be seen that the simulation results are in good agreement with the correlation calculation results, and the errors are small, all within 20%. The smallest error is approximately 7%. In the comparison of the data results, the simulation results had less error with the experimental data, so the simulation method was found to be reliable and universal.

2.4 Grid Independence Verification

The independence of the grids was verified by selecting five representative grid quantities for the 3D model previously used for verification, namely 1.7×10^6 grid (sparse), 2.6×10^6 grid (sparser), 3×10^6 grid (denser), 4×10^6 grid (denser), and 5×10^6 grid (very dense).

As shown in Figure 4, it can be seen that the j factor tends to fluctuate and the f factor tends to decrease with an increase in the number of grids, but the magnitude of the changes is small. Therefore, to save computational

time and to consider the accuracy of the simulation, 2.6×10^6 meshes were used for the calculation.

2.5 CFD Data

The orthogonal test is a design method for simultaneously studying multiple factors and multiple levels at the same time. This method selects some typical combinations of factors and levels from all the tests to study, and by studying few combinations, it can quickly understand the whole, which can not only improve the efficiency of the study, but also reduce the cost of the study.

The three structural parameters of louver angle θ , fin length a , and louver pitch L_p were used as experimental factors with six levels in this study, and each factor and its level are shown in Table 2.

After the mesh is divided, the boundary conditions must be set using Fluent. A reasonable boundary condition can make the simulation results more accurate and improve the efficiency of the simulation. The specific boundary conditions were set as follows.

1. The inlet is set as a velocity inlet with air flow velocities of 2 m/s, 4 m/s, 6 m/s and 8 m/s and a constant temperature of 300 K.
2. The outlet was the pressure outlet, and the default gauge pressure was 0 Pa.
3. The wall of the flat tube is set as a thermostatic wall with a temperature of 363 K, and a thin shell is set for heat transfer with a thickness of 0.25 mm.
4. The rest of the wall surface, except for the fluid-solid contact surface, is adiabatic.
5. The turbulence model adopted the SST $k-\omega$ model, the pressure-velocity coupling adopted a coupled algorithm, the second-order windward format was chosen to discretize the basic control equations, and the convergence residuals of energy and momentum were set to be less than 10^{-6} .

The fluid in this simulation was air, the solid was a fin and flat tube, and the material used was aluminum. Their physical parameters are listed in Table 3.

3 Description of the Artificial Neural Network Model

Artificial neural network (ANN) is an adaptive nonlinear dynamic system composed of many interconnected neurons. They can classify data using the network's own memory and analysis, and the accuracy of the model prediction results can be ensured through correlation processing. In addition, the unique structure, adaptive learning, memory, strong fault tolerance, and robustness

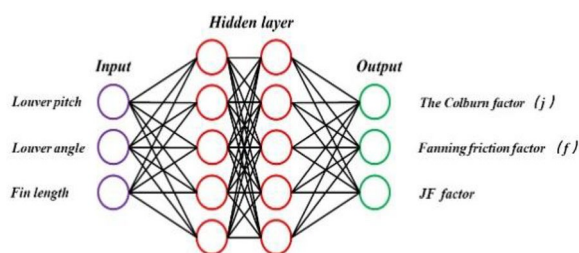


Figure 5 Schematic diagram of neural network structure

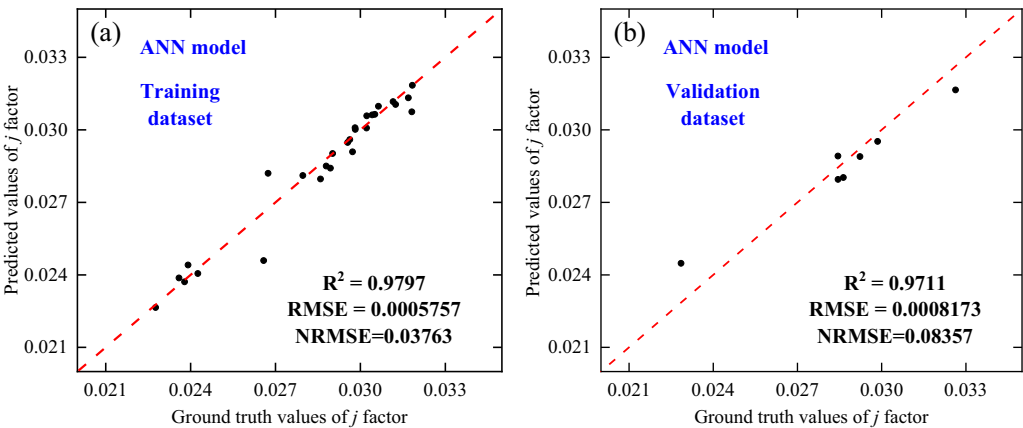


Figure 6 Comparison of predicted and simulated values of j factor

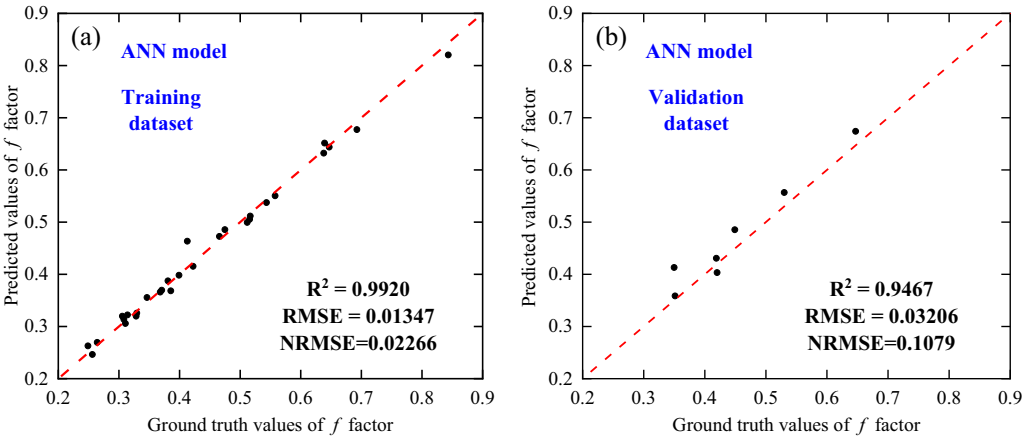


Figure 7 Comparison between predicted and simulated values of f factor

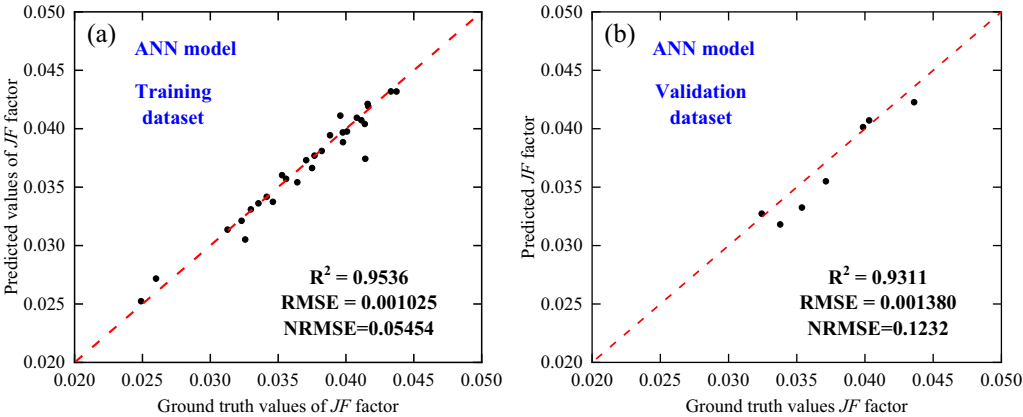


Figure 8 Comparison of predicted and simulated values of Jf factor

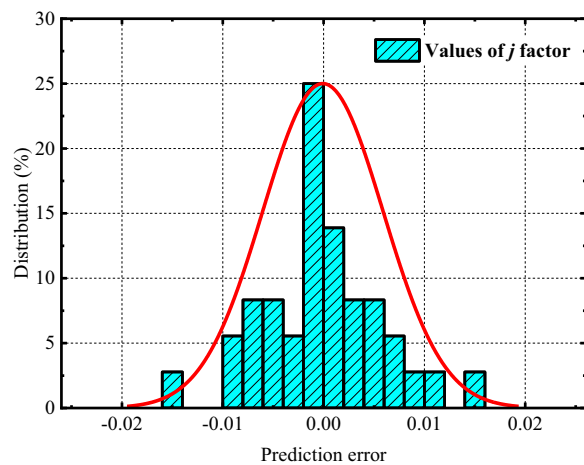


Figure 9 Absolute error distributions of j factor prediction

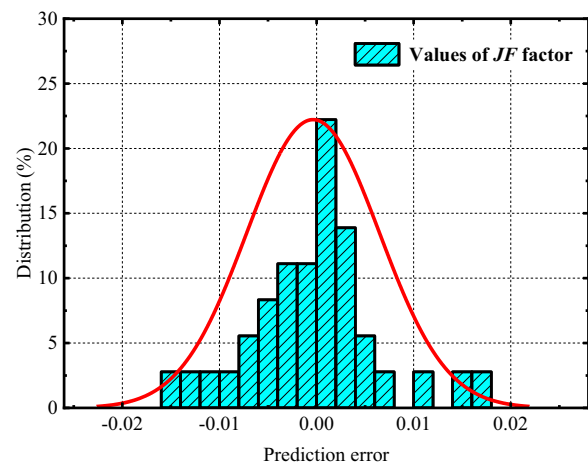


Figure 11 Absolute error distributions of JF factor prediction

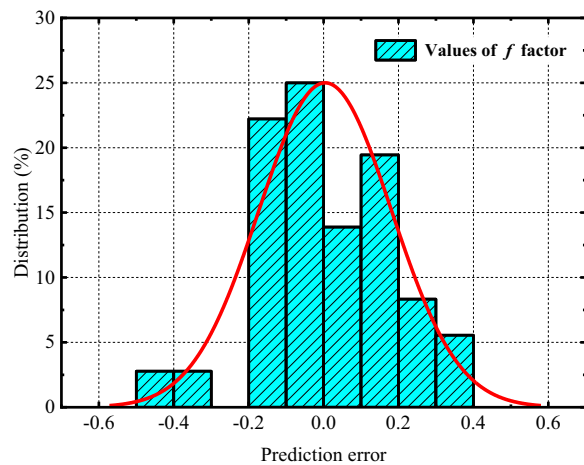


Figure 10 Absolute error distributions of f factor prediction

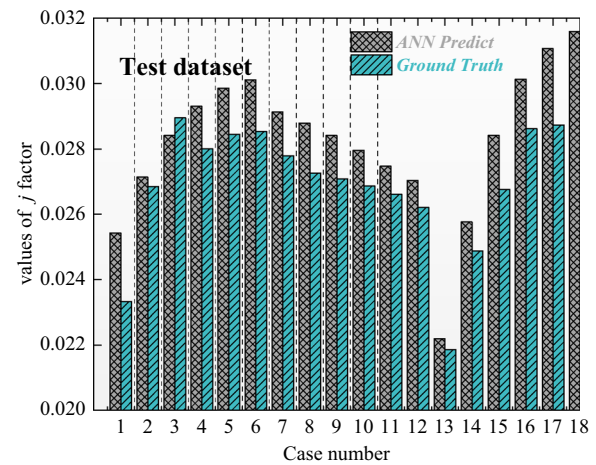


Figure 12 Comparison of predicted and actual values of the j factor

of neural networks make them widely used in the field of prediction.

The process of machine learning can be briefly summarized as follows: First, a large amount of data is used to train the model, then the model is trained by iterating the error of the model on the dataset continuously to obtain a model that fits reasonably well to the dataset, and finally, the trained model can be put into practical application. To reduce the generalization error of the trained model, we need to divide the dataset into a test set and a training set. The data in the training set is used to train the model, and the error of the model in the test set can be approximated as a generalization error; thus, the generalization error can be reduced by only reducing the error of the model in the test set.

The 36 sets of data provided by the previous CFD were divided into training and validation sets. Among them, 80% (29/36) of the training set was randomly selected

from the simulation data containing the working points under various conditions. The remaining 20% (7/36) were selected as the training set to validate the accuracy of the machine learning prediction model.

The flow heat transfer performance of the louvered fins is affected by structural parameters such as louver angle, fin length, and louver spacing, which is a multivariate nonlinear complex system. Thus, a BP neural network capable of good prediction performance is established, as shown in Figure 5, to predict the flow heat transfer in louvered fins. In a BP neural network, the weight and deviation vectors are trained using a gradient descent algorithm, which can be better. During the supervised learning process, the learning rate was 0.01 and the minimum error of the training target was 0.001.

When building the neural network model, random was used for the data partitioning algorithm, Levenberg-Marquardt was used for the training algorithm, Mean

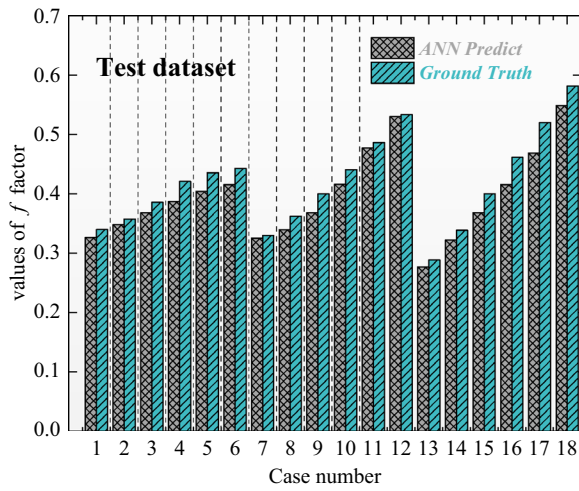


Figure 13 Comparison of predicted and actual values of the f factor

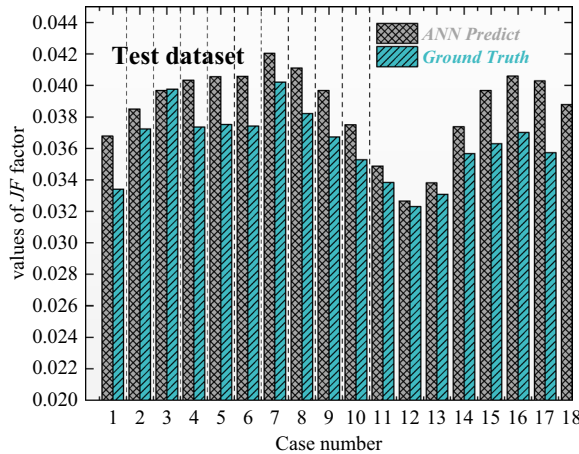


Figure 14 Comparison of predicted and actual values of the JF factor

Squared Error was used for the error algorithm, and MEX was used for the compilation algorithm. The maximum number of training iterations of the model was 1000, and the target error was 0.001.

When building the neural network model, random was used for the data partitioning algorithm, Levenberg-Marquardt was used for the training algorithm, Mean Squared Error was used for the error algorithm, and MEX was used for the compilation algorithm. The maximum number of training iterations of the model was 1000, and the target error was 0.001.

For the evaluation metrics, the coefficient of determination (R^2) and root mean square error ($RMSE$) are used to measure the prediction performance of the established neural network for the above three

metrics. If R^2 is very close to 1 and the $RMSE$ value is very small, it indicates that the model can learn the data very well; to exclude the effect of the data itself being too small on the $RMSE$ accuracy, it can be normalized and the $NRMSE$ can be used to replace the role of the $RMSE$. The expressions for R^2 , $RMSE$, and $NRMSE$ are shown in Eqs. (15)–(17):

$$R^2 = \frac{\sum_{i=1}^n (\hat{y}_i - \bar{y})^2}{\sum_{i=1}^n (y_i - \bar{y})^2}, \quad (15)$$

$$RMSE = \sqrt{\frac{1}{n} \sum_{i=1}^n |y_i - \hat{y}_i|^2}, \quad (16)$$

$$NRMSE = \frac{RMSE}{y_{\max} - y_{\min}}, \quad (17)$$

where \hat{y}_i is the predicted data, \bar{y} is the average of the measured data, y_i is the simulated data, y_{\max} is the maximum value of the measured data, y_{\min} is the minimum value of the measured data, and n is the number of data.

4 Results and Discussion

4.1 Neural Network Performance Evaluation

This section presents the ANN model for predicting the flow heat transfer performance of louvered fins, including the heat transfer factor j , resistance factor f , and the overall performance rating factor JF .

Figures 6, 7, 8 show the actual values of the training dataset compared with the prediction results of the ANN-based model. The figure shows that all points in the graph of the neural network prediction model are very close to the diagonal line, which indicates that the neural network model has a good prediction performance. The R^2 values of j , f , and JF in the training and validation sets are 0.9797, 0.9920, 0.9536, 0.9711, 0.9647, and 0.9311, respectively, and the $NRMSE$ s are 0.03763, 0.02266, 0.05454, 0.08357, 0.1079, and 0.1232, respectively. An R^2 value close to 1 indicates that the ANN model can learn the intrinsic relationship between the louvered fin structure parameters and the flow heat transfer performance.

The accuracy of the machine learning prediction performance was determined by measuring the distance between the data points on the graph and diagonal line. As can be seen in Figure 6(a), the points of the ANN prediction model are relatively close to the 45° line, which indicates good agreement between the prediction model results and the experimental simulation data. Therefore, all the results indicate that the ANN has good generalization ability in the prediction of heat transfer in louvered

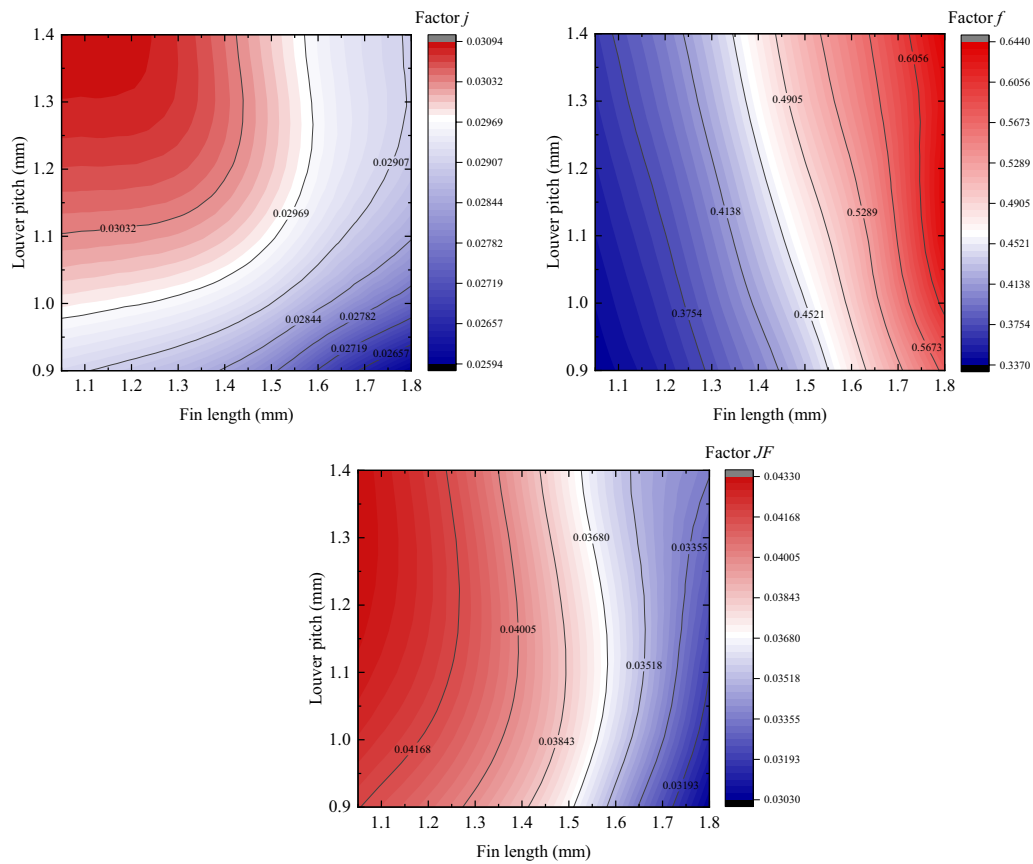


Figure 15 Change trend of j , f and JF factors when louver angle is 25°

fin flow, and the model can learn the internal connections between the relevant parameters of the training data better. In general, the R^2 values were close to 1, indicating that the ANN model successfully learned the relationship between the geometric parameters of the louvered-fin cross-section and its flow heat transfer performance. If properly trained, the errors are acceptable.

Figures 9, 10, 11 show the absolute errors between the ANN prediction results and the simulation data of the louvered fins, which can be used to analyze the error distribution of the model training. It can be found that the error interval of the neural network model is very close to the normal distribution, indicating that the error of this neural network model is concentrated around $x = 0$. The absolute error takes the middle line of the normal curve as the symmetry axis, and the distribution of the absolute error gradually and uniformly decreases to the left and right, respectively. The absolute error distributions of the j factor, f factor, and JF factor in the neural network model and simulation data were $-0.02 \sim 0.02$, $-0.5 \sim 0.4$, and $-0.02 \sim 0.02$, respectively. The prediction errors in

the training set were more concentrated around $x = 0$ than those in the validation set.

To further evaluate the learning degree of the trained artificial neural network model on the relationship between the louvered-fin structure parameters and performance, 18 groups of experimental data were selected as the test sets, and the j , f , and JF values predicted by the ANN model were compared with the simulated Ground Truth data of the test set. The results are shown in Figures 12, 13, 14. By analyzing the data in the figures, it can be found that the difference between the predicted value and the simulation value of the j and f factors in the test set is within 10%, among which the error of more than half of the j factor is within 5%, and the error of more than 40% of the f factor is within 5%. As the JF factor is calculated using j and f , the error is large. However, these values were within 12%. It can be observed from the three figures that the predicted values are in good agreement with the simulation values, which further confirms the reliability of the ANN model.

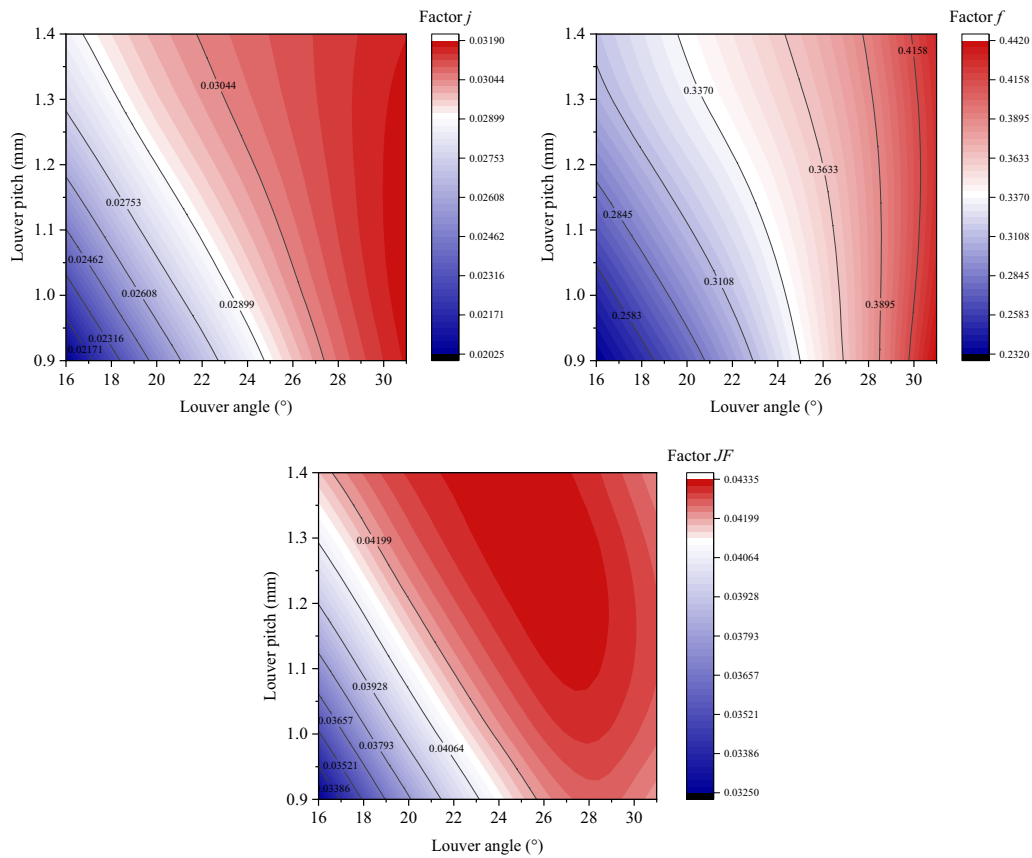


Figure 16 Change trend of j , f and JF factors when fin length is 1.05 mm

4.2 Structure Optimization

In this study, we investigated the influence of three structural parameters, namely louver angle, fin length, and louver pitch, on the performance of louvered fins and optimized the structure. This process is not only time-consuming but also consumes considerable resources, and the repetitive process is tedious to the operators. In this section, the trained artificial neural network model only needs to input the structural parameters of 216 models to output the corresponding j , f , and JF factors of the models, and the structural parameters of the model with the largest JF factor can be found to perform structural optimization.

After inputting 216 sets of structural parameters, the structural parameters with the largest set of JF factors in the output data are louver angle $\theta = 25^\circ$, fin length $a = 1.05$ mm, and louver pitch $L_p = 1.3$ mm. The j , f , and JF factors of this structure are 0.0308, 0.3618, and 0.0433, respectively. The j factor of the initial model is 0.0285, the f factor is 0.5322, and the JF factor is 0.0351. This model improved the heat transfer factor j by 2.87%, reduced the friction factor f by 30.4%, and improved the

overall performance factor JF by 15.7% compared to the initial model.

To demonstrate the plausibility of the optimization, 216 sets of data output from the neural network model can be analyzed in relation to the structural parameters of the louvered fins to determine whether they are consistent with the flow and heat transfer laws simulated by the simulation.

From the 216 sets of data, the louver angle $\theta = 25^\circ$, the fin length $a = 1.05$ mm, and the louver pitch $L_p = 1.3$ mm were selected to plot the variation of the evaluation index with the other two structural parameters when changing a certain structural parameter. As shown in Figures 15, 16, 17.

When the louver angle $\theta = 25^\circ$, it can be seen from the figure that when the fin length is certain, with the increase of the louver spacing, j factor and f factor are gradually increased, and JF factor is first increased and then decreased; when the louver spacing is certain, with the increase of the fin length, j factor and JF factor are gradually decreased, and f factor is gradually increased.

According to these figures, it is apparent that when the fin length a is 1.05 mm and the louver spacing is fixed,

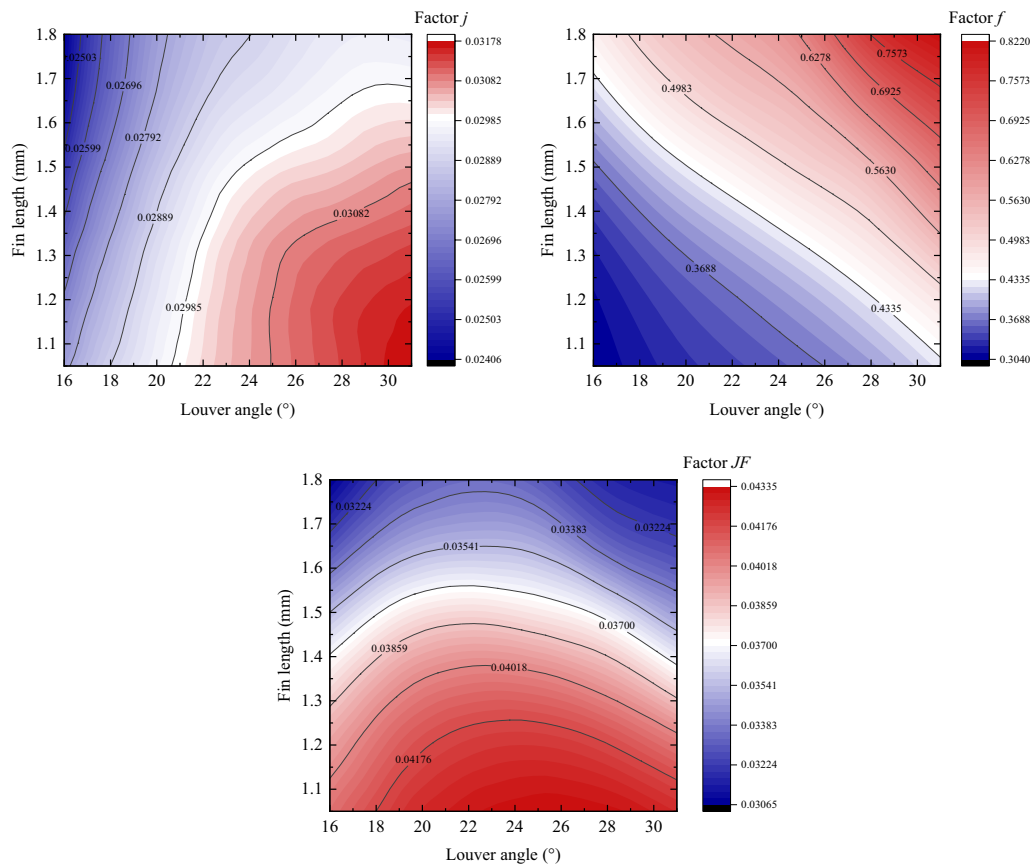


Figure 17 Change trend of j , f and JF factors when louver spacing is 1.3 mm

an increase in louver angle causes a gradual increase in both the j factor and f factor. Meanwhile, the JF factor initially increases but subsequently decreases. If the louver angle is held constant, increasing the louver spacing yields gradual increases in the j factor, f factor, and JF factor when the louver angle is small. However, when the louver angle is large, increasing the louver spacing results in a gradual increase in the j factor, an increase followed by a decrease in the JF factor, and a decrease followed by an increase in the f factor.

When the louver pitch is 1.3 mm, if the fin length is certain, with an increase in the louver angle, the j factor and f factor will gradually increase, and the JF factor will first increase and then decrease; if the louver angle is certain, with the increase in the fin length, the j factor gradually decreases, the f factor will gradually increase, and the JF factor will gradually decrease.

Through the above analysis, it can be observed that the heat transfer and flow laws of the neural network predicted data are roughly consistent with those of the 36 sets of simulated data in the orthogonal tests in Section 4 of this study, which indicates that the optimization

results of the neural network model in this study have a high degree of confidence.

5 Conclusions

The aim of this study was to evaluate whether the ANN model can be used to predict the flow and heat transfer capacity of a louvered-fin heat exchanger and to optimize the louvered-fin structure. The results showed that the predicted j factor, f factor, and JF factor agreed well with the simulated values, and the predicted trends for the different indicators were the same as the true pattern. This indicates that the machine prediction model can learn the relationship between the three structural parameters of louver angle, fin length, and louver spacing on the flow heat transfer of the louvered fins from a series of linearly uncorrelated data. Because laboratory measurements are expensive and difficult to measure accurately and numerical simulations are demanding and time-consuming, the use of neural network models to assist laboratory measurements or numerical simulations to analyze the flow and heat transfer performance can reduce the number and cost of experimental cases and significantly reduce time costs. The application of

artificial neural network models in the field of louvered fins is beneficial for the progress and optimization of louvered fins.

Therefore, it is of great significance to improve the heat dissipation performance of vehicle radiators to obtain satisfactory performance for special vehicles running in plateau areas.

Acknowledgements

Not applicable.

Author contributions

CL was in charge of the whole trial; HG wrote the manuscript; XS and YZ assisted with sampling and laboratory analyses. All authors read and approved the final manuscript.

Authors' Information

Chunming Li, born in 1964, received the Ph.D. degree from *Beijing Institute of Technology, China*, in 2011. He is currently the head technology principal of *China North Vehicle Research Institute*. His current research interests include the vehicle overall performance matching, power management, and control strategy optimization. E-mail: chunming@noveri.com.cn

Xiaoxia Sun, born in 1983, received the Ph.D. degree from *Beijing Institute of Technology, China*, in 2011. She is currently a researcher of *China North Vehicle Research Institute*. Her current research interests include the vehicle power management, thermal management, and control strategy optimization. E-mail: sun_xiaoxia1983@163.com

Hongyang Gao, born in 1999, received the bachelor's degree in mechanical engineering from *Zhejiang University City College, China*, in 2022. He is currently pursuing a master's degree at *Zhejiang University of Technology*. E-mail: 31903121@stu.zucc.edu.cn

Yu Zhang, born in 1983, received the Ph.D. degree in engineering thermo-physics from *Zhejiang University, China*, in 2013. He is currently an associate professor of *Zhejiang University City College*. He has long been committed to the combustion mechanism of internal combustion engines, in-cylinder heat transfer mechanism, flow and heat transfer mechanism of heat exchangers, hybrid vehicle thermal management technology, machine learning algorithm, etc. E-mail: zhangyu_gcxy@zucc.edu.cn

Funding

Supported by Zhejiang Provincial Natural Science of China (Grant No. LQ20E060003), Zhejiang Provincial Basic Public Welfare Research Project of China (Grant No. LGG20E050007), Key Projects of Hangzhou Agricultural and Social Development Research Program of China (Grant No. 20212013B04), Projects of Hangzhou Agricultural and Social Development Research Program of China (Grant Nos. 20201203B128, 20212013B04), Scientific Research Foundation of Zhejiang University City College of China (Grant Nos. J-202116, X-202205), and 2021 Teacher Professional Development Program for Domestic Visiting Scholars in Universities of China (Grant No. FX2021105).

Availability of data and materials

The datasets supporting the conclusions of this article are included within the article.

Ethics approval and consent to participate

Not applicable

Consent for publication

Not applicable

Competing interests

The authors declare no competing financial interests.

Received: 24 June 2022 Revised: 1 March 2023 Accepted: 7 March 2023

Published online: 06 April 2023

References

- [1] Z Liu, J Liu. Effect of altitude conditions on combustion and performance of a turbocharged direct-injection diesel engine. *Proceedings of the Institution of Mechanical Engineers, Part D: Journal of Automobile Engineering*, 2021, 236(4): 582-593.
- [2] X Wang, Y Ge, L Yu, et al. Effects of altitude on the thermal efficiency of a heavy-duty diesel engine. *Energy*, 2013, 59: 543-548.
- [3] Z Kan, Z Hu, D Lou, et al. Effects of altitude on combustion and ignition characteristics of speed-up period during cold start in a diesel engine. *Energy*, 2018, 150: 164-175.
- [4] C Zhang, Y Li, Z Liu, et al. An investigation of the effect of plateau environment on the soot generation and oxidation in diesel engines. *Energy*, 2022, 253: 124086.
- [5] A Kumar, M A Hassan, P Chand. Heat transport in nanofluid coolant car radiator with louvered fins. *Powder Technology*, 2020, 376: 631-642.
- [6] M Zeeshan, S Nath, D Bhanja. Numerical study to predict optimal configuration of fin and tube compact heat exchanger with various tube shapes and spatial arrangements. *Energy Conversion and Management*, 2017, 148: 737-752.
- [7] C C Wang, K Y Chen, J S Liaw, et al. An experimental study of the air-side performance of fin-and-tube heat exchangers having plain, louver, and semi-dimple vortex generator configuration. *International Journal of Heat and Mass Transfer*, 2015, 80: 281-287.
- [8] C Cuevas, D Makaire, L Dardenne, et al. Thermo-hydraulic characterization of a louvered fin and flat tube heat exchanger. *Experimental Thermal and Fluid Science*, 2011, 35(1): 154-164.
- [9] M Ferrero, A Scattina, E Chiavazzo, et al. Louver finned heat exchangers for automotive sector: Numerical simulations of heat transfer and flow resistance coping with industrial constraints. *Journal of Heat Transfer*, 2013, 135(12): 121801.
- [10] Y Y Liang, C C Liu, C Z Li, et al. Experimental and simulation study on the air side thermal hydraulic performance of automotive heat exchangers. *Applied Thermal Engineering*, 2015, 87: 305-315.
- [11] E M Cardenas Contreras, E P Bandarra Filho. Heat transfer performance of an automotive radiator with MWCNT nanofluid cooling in a high operating temperature range. *Applied Thermal Engineering*, 2022, 207: 118149.
- [12] L Garelli, G Ríos Rodríguez, J J Dorella, et al. Heat transfer enhancement in panel type radiators using delta-wing vortex generators. *International Journal of Thermal Sciences*, 2019, 137: 64-74.
- [13] R R Sahoo, P Ghosh, J Sarkar. Energy and exergy comparisons of water based optimum brines as coolants for rectangular fin automotive radiator. *International Journal of Heat and Mass Transfer*, 2017, 105: 690-696.
- [14] K Ryu, S J Yook, K S Lee. Optimal design of a corrugated louvered fin. *Applied Thermal Engineering*, 2014, 68(1): 76-79.
- [15] K Ryu, K S Lee. Generalized heat-transfer and fluid-flow correlations for corrugated louvered fins. *International Journal of Heat and Mass Transfer*, 2015, 83: 604-612.
- [16] J Y Jang, C C Chen. Optimization of louvered-fin heat exchanger with variable louver angles. *Applied Thermal Engineering*, 2015, 91: 138-150.
- [17] J S Park, D R Kim, K S Lee. Frosting behaviors and thermal performance of louvered fins with unequal louver pitch. *International Journal of Heat and Mass Transfer*, 2016, 95: 499-505.
- [18] B Ameel, J Degroote, C T'Joen, et al. Optimization of x-shaped louvered fin and tube heat exchangers while maintaining the physical meaning of the performance evaluation criterion. *Applied Thermal Engineering*, 2013, 58(1): 136-145.
- [19] H M Ali, W Arshad. Thermal performance investigation of staggered and inline pin fin heat sinks using water based rutile and anatase TiO₂ nanofluids. *Energy Conversion and Management*, 2015, 106: 793-803.
- [20] M Khoshvaght-Aliabadi, F Hormozi, A Zamzamin. Effects of geometrical parameters on performance of plate-fin heat exchanger: Vortex-generator as core surface and nanofluid as working media. *Applied Thermal Engineering*, 2014, 70(1): 565-579.
- [21] R L Webb, P Trauger. How structure in the louvered fin heat exchanger geometry. *Experimental Thermal and Fluid Science*, 1991, 4(2): 205-217.
- [22] P A Sanders, K A Thole. Effects of winglets to augment tube wall heat transfer in louvered fin heat exchangers. *International Journal of Heat and Mass Transfer*, 2006, 49(21): 4058-4069.
- [23] M H Park, S C Kim. Heating performance enhancement of high capacity PTC heater with modified louver fin for electric vehicles. *Energies*, 2019, 12(15): 2900.

- [24] L B Erbay, N Uğurlubilek, Ö Altun, et al. Numerical investigation of the air-side thermal hydraulic performance of a louvered-fin and flat-tube heat exchanger at low Reynolds numbers. *Heat Transfer Engineering*, 2017, 38(6): 627-640.
- [25] C T Hsieh, J Y Jang. Parametric study and optimization of louver finned-tube heat exchangers by Taguchi method. *Applied Thermal Engineering*, 2012, 42: 101-110.
- [26] J Deng. Improved correlations of the thermal-hydraulic performance of large size multi-louvered fin arrays for condensers of high power electronic component cooling by numerical simulation. *Energy Conversion and Management*, 2017, 153: 504-514.
- [27] Z Qian, Q Wang, J Cheng, et al. Simulation investigation on inlet velocity profile and configuration parameters of louver fin. *Applied Thermal Engineering*, 2018, 138: 173-182.
- [28] H Peng, X Ling. Optimal design approach for the plate-fin heat exchangers using neural networks cooperated with genetic algorithms. *Applied Thermal Engineering*, 2008, 28(5): 642-650.
- [29] H K Aasi, M Mishra. Experimental investigation and ANN modelling on thermo-hydraulic efficacy of cross-flow three-fluid plate-fin heat exchanger. *International Journal of Thermal Sciences*, 2021, 164: 106870.
- [30] T A Tahseen, M Ishak, M M Rahman. Performance predictions of laminar heat transfer and pressure drop in an in-line flat tube bundle using an adaptive neuro-fuzzy inference system (ANFIS) model. *International Communications in Heat and Mass Transfer*, 2014, 50: 85-97.
- [31] J Liu, H Wang. Machine learning assisted modeling of mixing timescale for LES/PDF of high-Karlovitz turbulent premixed combustion. *Combustion and Flame*, 2022, 238: 111895.
- [32] J Liu, Q Huang, C Ulishney, et al. Machine learning assisted prediction of exhaust gas temperature of a heavy-duty natural gas spark ignition engine. *Applied Energy*, 2021, 300: 117413.
- [33] Y Zhang, Q Wang, X Chen, et al. The prediction of spark-ignition engine performance and emissions based on the SVR algorithm. *Processes*, 2022, 10(2): 312.
- [34] J Fu, R Yang, X Li, et al. Application of artificial neural network to forecast engine performance and emissions of a spark ignition engine. *Applied Thermal Engineering*, 2022, 201: 117749.
- [35] J Wen, K Li, C Wang, et al. Optimization investigation on configuration parameters of sine wavy fin in plate-fin heat exchanger based on fluid structure interaction analysis. *International Journal of Heat and Mass Transfer*, 2019, 131: 385-402.
- [36] M A Alfellag, H E Ahmed, A S Kherbeet. Numerical simulation of hydro-thermal performance of minichannel heat sink using inclined slotted plate-fins and triangular pins. *Applied Thermal Engineering*, 2020, 164: 114509.
- [37] Y J Chang, C C Wang. A generalized heat transfer correlation for louver fin geometry. *International Journal of Heat and Mass Transfer*, 1997, 40(3): 533-544.
- [38] Y J Chang, K C Hsu, Y T Lin, C C Wang. A generalized friction correlation for louver fin geometry. *International Journal of Heat and Mass Transfer*, 2000, 43(12): 2237-2243.

Submit your manuscript to a SpringerOpen[®] journal and benefit from:

- Convenient online submission
- Rigorous peer review
- Open access: articles freely available online
- High visibility within the field
- Retaining the copyright to your article

Submit your next manuscript at ► [springeropen.com](https://www.springeropen.com)